Iranian Journal of Physics Research, Vol. 23, No. 3, 2023
DOI: 10.47176/ijpr.22.3.71726

Investigation of ultra-high energy cosmic ray mass composition by the ground based detectors

S Doostmohammadi
Faculty of Physics, Shahid Bahonar University of Kerman, Kerman, Iran

E-mail: doostmohammadi@uk.ac.ir

(Received 16 July 2023 ; in final form 10 August 2023)

Abstract
Mass composition of cosmic rays and thus determining their sources, especially at high energies, is one of the most important parts of astroparticle physics and cosmic ray science which also can help to know the universe better. Many different methods have been used to estimate the mass composition so far, which the most important of them has been done by Pierre Auger observatory group. In present work, in order to estimate the mass composition of cosmic rays, two different ways (first using from muonic component and second, maximum atmospheric depth) are used which they have been done by comparing experimental data and simulated ones. An increase in the mass composition and low flux of photons is observed at high energies. The diagram of maximum atmospheric depth in terms of energy, which is produced by extrapolation and interpolation statistical method, raises and falls meaningfully that is compatible to the results of Pierre Auger observatory. At higher energies, the percentage of primary particles have a tendency to heavier particles and in low energies the primary particles are lighter. Also, the most important breaks in the energy spectrum of cosmic rays are seen.

Keywords: cosmic ray, extensive air shower, mass composition, maximum atmospheric depth

1. Introduction

The collision of cosmic rays (CR) with energies above 10^{13} eV to atmospheric molecules and atoms causes the formation of cascades of light particles such as muons, protons, pions, electrons and etc which is called extensive air showers (EAS). These EAS consist of three main components: electromagnetic, muonic and hadronic. Each of these components provide important information about the characteristics of primary particles such as mass composition (MC), energy and their arrival direction. The electromagnetic component represents the largest part of the EAS and accounts for 90% of the total primary energy. This component includes electrons, positrons and gamma rays which are usually made of decaying neutral pions over two gammas. The main parts of the hadronic component are kaons and pions. These particles remain near the axis of the EAS [1 - 4]. Most of the particles that reach the Earth's surface are muons, about a hundred particles per square meter per second at energies around 10^{18} eV. The muonic component is the result of the decay of unstable mesons, such as charged pions. Muons are highly permeable particles that because of their relativistic behaviors, have a relatively long lifetime much longer than many other subatomic particles. On the other hand, muons have a very small cross-sectional area and therefore can reach the ground level and even penetrate the earth and be detected by underground detectors. The number of muons that reach the ground is sensitive to the type of primary particle [5 - 6]. In low energy, MC is measured directly by the detectors at the top of the atmosphere, but in high energy, the MC of CRs must be measured indirectly [7].

Estimating the MC of CRs in high energies has been done in many different ways, the most important of which have been provided by Pierre Auger Observatory group [8].

Pierre Auger Observatory is a very powerful group in the field of CRs science because of their surface detectors and fluorescent telescopes, which provides many useful information about MC of ultra-high energy CRs [8]. In the most of Auger's researches, estimation of MC is derived from maximum atmospheric depth of EAS (Xmax; where the number of secondary particles such as electrons, positrons, muons and photons reaches to their maximum numbers) which is mostly obtained from fluorescence telescopes. Fluorescence telescopes measure emitted light which are produced in hitting secondary particles of EAS to atmospheric nitrogen molecules. The data from fluorescence detectors can provide the Xmax of each EAS

and thus one can estimate the MC of primary CR from some equations and parameters [9]. For example, in some studies [10], equation 1 is used, which is the relationship between the Xmax and the MC of the primary particle colliding the atmosphere molecules

$$\langle \ln A \rangle = \frac{\langle X_{\max}^{p} \rangle - \langle X_{\max}^{data} \rangle}{\langle X_{\max}^{p} \rangle - \langle X_{\max}^{Fe} \rangle} \ln 56, \quad (1)$$

at which $\langle X_{\max}^{p} \rangle$ and $\langle X_{\max}^{Fe} \rangle$ are maximum atmospheric depth of proton and iron respectively, A and $\langle X_{\max}^{data} \rangle$ are the mass number and Xmax of the primary particle, respectively. Finally, the results of Auger group prove that the evolution and progression of MC toward lighter nuclei (up to the energy of $10^{18.27}$ eV). At energies above $10^{18.27}$ eV, the reverse process is happening and MC becomes heavier so that this fluctuation can be seen in figure 1 [11]. At present work, the MC of CRs has been investigated in high energy range (10^{17} eV to 10^{20} eV) by comparing the simulation results to the Auger Observatory experimental data [12].

2. Muonic component of EAS

The muonic component of EAS is usually caused by the decay of positive and negative pions. When primary heavy particles, such as iron nuclei, hit to the earth atmosphere nuclei, break down into their nucleons and in result of more multiplicity, they have much more muon than lighter particles such as protons and gamma rays. In this study, due to simulation data by Corsika - 77420 program [13] (QGSJET01 [14] for high energy and GHEISHA [15] for low energy) and calculation of Xmax versus energy by some statistical methods and finally comparison with experimental data, estimation of MC of CRs in high energies is investigated.

In the classic framework, the lifetime of muons is 2.2 microseconds and they decay after traveling a distance of 660 meters. But, if muons move at a rate of 99.8% of the speed of light, (which occur in EAS) according to a special relativity theory, they can reach the ground from a higher height of above the ground [16]. Here, the comparison of experimental and simulation data is used. For this purpose, 200 experimental data have been selected from Auger data, each of which has a median density, the initial energy of the particles and the arrival direction of the particles. The energy range of these EAS is selected in the range of 10^{17} eV to 10^{20} eV and for the zenith angle of EAS from 0 to 60 degrees, and each of them has a specific diagram of the average density in terms of distance from the EAS core.

First, the experimental data are extracted from a diagram of each EAS and the number of electrons (Ne) is calculated, based on the theory of electromagnetic cascades, from equation 1, the NKG function [17 – 18]

$$p(N_e, r) = \frac{N_e}{2\pi r_M^2} \left(\frac{r}{r_M}\right)^{s-2} \left(1+\frac{r}{r_M}\right)^{s-4.5} \left(\frac{\Gamma(4.5-s)}{\Gamma(s)\Gamma(4.5-2s)}\right), \quad (2)$$

where p is the density, N_e is shower size, r_M is Moliere radius which is depend on environmental situations, r is core distance and s (wich has no unit) is the age parameter.

Then equation 2 is used to calculate the number of Muons per EAS [19]

$$N_\mu = (2.94 \pm 0.141) \times 10^5 \times \left(\frac{N_e}{10^7}\right)^{(0.76\pm0.02)}, \quad (3)$$

These steps are performed for two hundred experimental data, as shown in Table 1 for a few EAS as instance.

To compare with the experimental data, simulation data were used so that proton, gamma and iron in three energy of 10^{17} eV, 10^{18} eV and 10^{19} eV and in the optional arrival directions were simulated. For each energy and for each particle, five hundred data and in total about one thousand and five hundred data were simulated.

According to the obtained results and after the necessary averaging of simulation data, the diagram of the number of muons of each EAS is drawn in terms of energy. As shown in figure 2, the black dots are experimental data and the lines are the value of simulated ones.

As expected, at high energies the number of muons of heavy particles such as iron is much more significant than of lighter particles such as protons and also gamma rays. Also, at high energies, the percentage of primary photons is very low which is seen in figure 2. According to the results of comparing of simulated and experimental data, it can be said that in high energy range (10^{17} eV to 10^{20} eV) a relative increase in percentage of MC is seen. Due to the existence of two scenarios about the percentage of photon in primary CRs (top-down or non-accelerated theory which predicts the percentage of photons up to 50% and bottom-up theory that predicts this percentage very low) [20-22] the results of this study and percentage of obtained photons, is compatile to the bottom-up theory.

3. Maximum atmospheric depth of extensive air showers

When a primary energetic particle enters the Earth's atmosphere, the first interaction with the atmospheric nuclei usually occurs at an altitude of 10 to 40 km. With the longitudinal expansion of the EAS in the atmosphere, the number of secondary particles increases until reaches to its maximum at a certain height. Conventionally, the value of the age parameter of an EAS is considered equivalent as one at Xmax. The age parameter value is less than one before Xmax and is more than one after Xmax. For the same primary particles with the same arrival directions, the number of secondary particles produced by higher energetic primary particles is more. Also, for heavier nuclei in the same energy and the same arrival directions, the probability of collisions and interactions increase and thus the secondary particles reach to their maximum number at lower depth.

At ground level, the lower age parameter indicates that the number of particles, reaching the ground, increase and then such EAS is considered as young showers [23-24], so lighter particles penetrate to the earth atmosphere more than heavier particles. In other words, heavier particles, due to their collision cross-section and also their bigger nuclei, have more interactions with atmospheric particles and as a result, they have the lower Xmax. As mentioned above, the Pierre Auger observatory uses fluorescence telescopes and surface detectors to measure the Xmax, which has previously been discussed about the number of their corresponding simulated data and Xmax, produced in this study.

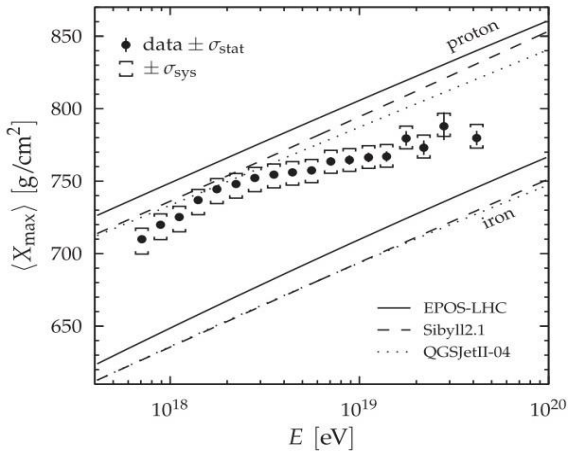

Figure 1. Average of Xmax of shower vs. energy compared to simulated data, done by A. Aab et al. [11].

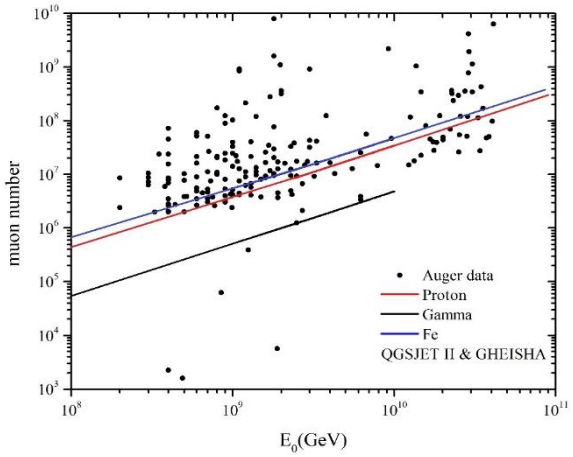

Figure 2. Comparison of experimental and simulation data.

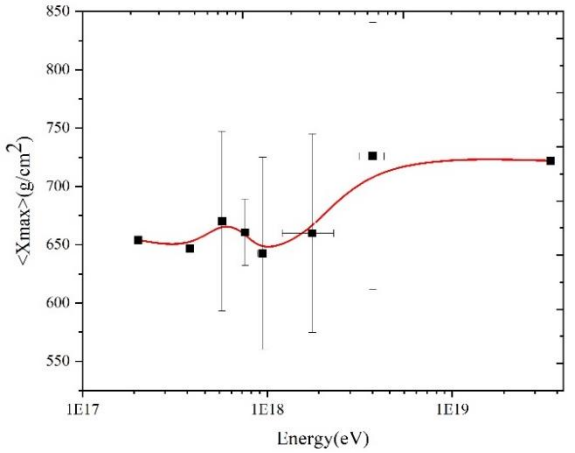

Figure 3. Xmax diagram in terms of energy for experimental data.

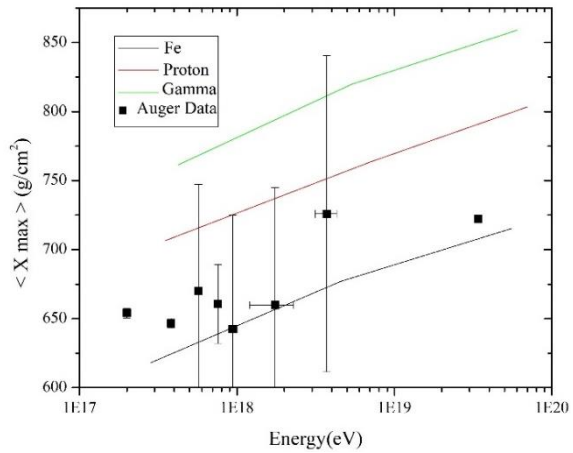

Figure 4. Comparison of the mean Xmax of our experimental data to simulation one.

Table 1. Example of Auger experimental data.

E(Eev)	Θ(deg)	s	Ne	N muon
0.4	44.4	1.471708	6.31E+08	6.89E+06
0.6	40.6	1.211059	2.84E+09	2.16E+07
0.85	53.3	3.133654	1298748	6.23E+04
1.67	31.51	1.273439	5.40E+09	3.52E+07
0.52	34.03	1.737473	3.01E+08	3.93E+06

The main method which is used at this study, is a statistical method that we used from extrapolation and interpolation of our simulated data to experimental data. In this way we obtain a relation among our simulated data and extrapolate to experimental data (which their Xmax were not specified) to obtain their Xmax. We used data extrapolation and interpolation by some python code. First, we used the signal vs. core distance diagrams from auger public experimental data. By fitting the lateral distribution function on these diagrams, we determined the age parameter and shower size of each shower. The number of muons calculated for each shower from equation (2) as well. Also, we had some useful parameters such as primary energy and zenith angle of each experimental data. Some of these parameters is seen in table 1. Then, we used many simulated data (around 1000 data) to extract the same parameters (primary energy, zenith angle, shower size, age parameter and muon number). Another extra parameter that we had in simulated data is Xmax. Then by using some python codes and also using extrapolation and interpolation concepts, we merged the experimental and simulated data to infer the best value of Xmax for each experimental data. Here, the innovative method (because we don't have Xmax of experimental data and use from surface detectors only) is to study the MC of CRs according to the Xmax derived only from ground-based detectors data (200 EAS). These results are obtained by comparison with a large number of simulated events as indicated in figure 3. Also, by some statistical averaging methods, the diagram of mean Xmax of simulated data, which are one thousand data, is plotted in terms of energy for the three particles Proton, Iron and Gamma as it can be seen in figure 4. Finally, the obtained results are then compared with simulation data which is shown in figure 4.

As indicated in figure 3, MC of ultra-high energy CRs has significant fluctuations, as expected.

These fluctuations, especially at energies above 10^{18} eV, have a tendency to light particles and then has a tendency to heavy particles which is compatile to universal outcomes, especially auger results in figure 1, [11].

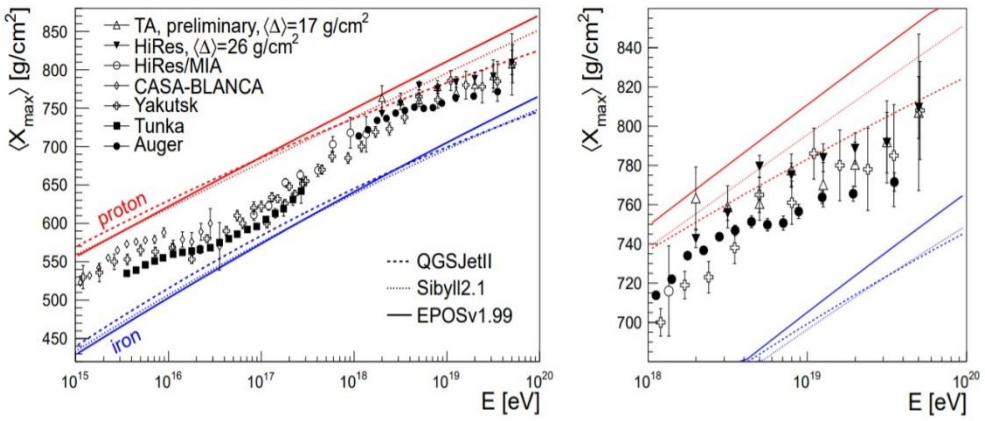

Figure 5. Results of the arrays of world-renowned detectors, done by K. H. Kampert and M. Unger [10].

As one can see in figure 4, at first, the average inclination of the experimental data is towards to heavy nuclei that this tendency is seen at energies above 10^{17} eV to about 2 $\times 10^{18}$ eV which is compatile tos the Auger results. But, at energies above 2 $\times 10^{18}$ eV, the tendency will change towards to light nuclei. This decrease in MC continues until the energy around 10^{19} eV and then, in higher energies, an increase in MC is observed again.

These results are in a good compatible with the data of the arrays of world-renowned detectors, as shown in figure 5 [10].

As it is seen in figure 5 and also was explained in the previous section, the fracture clearly shows the change in MC. If we look at the CRs energy spectrum, there is a fracture in the energy about 3 × 10^{18} eV so called the ankle. The reason of this fracture is a change in the MC of the primary CRs. As indicated in figure 4, at energy of ankle, this fracture is obviously seen so it can be concluded that the reason of this fracture and inclination to lighter nuclei is the change in high energy cosmic ray sources. As mentioned above, we used experimental data which are taken by auger detector array and the inclination of auger data to heavy particles at energies above 3 × 10^{18} eV in figure 5, is in a proper compatible with our results.

4. Conclusion

Regarding to muonic component of EAS, it is noteworthy that in the high energy range (10^{17} eV to 10^{20} eV) (10^{17} to 10^{20}) we are faced to an average relative increase in the percentage of MC and also the decrease of photon fraction. Due to the existence of two scenarios about the percentage of photons in CRs, the results of this study and the percentage obtained for high-energy photons, is compatible with the bottom-up scenario as well. Moreover, according to the obtained results from comparing of simulated and experimental data, it can be said that the average MC of primary cosmic rays has inclination to lighter particles to energy about $10^{18.3}$ eV, which is the same as the ankle energy of CRs energy spectrum. In the energy between $10^{18.5}$ and 10^{19} eV, it has been observed that the mass composition of the primary CRs has a tendency to heavy nuclei which is compatile with the Auger results too.

References

1. J Linsley, *Proc. 8th ICRC* **4** (1963) 77.
2. A M Hillas, *J. Phys*. **31** (2005) R95.
3. D Allard, E Parizot, and A V Olinto, *Astropart. Phys*. **27** (2007) 61.
4. R Aloisio, V Berezinsky, P Blasi, et. al., *Astropart. Phys*. **27** (2007) 76.
5. R Ulrich, R Engel, and M Unger, *Phys. Rev. D*, **83** (2011) 054026.
6. R Engel, D Heck, and T Pierog, *Ann. Rev. Nucl. Part. Sci*. **61** (2011) 467.
7. J Knapp, D Heck, S J Sciutto, M T Dova, and M Risse, *Astroparticle Physics*, **19** (2003) 77.
8. The Pierre Auger Collaboration, Nucl. Instrum. *Methods Phys. Res. A* **798** (2015) 172.
9. A Letessier-Selvon et al. (Pierre Auger Collab.), Proc. 33rd Int. Cosmic Ray Conf., Rio de Janeiro, Brazil (2013).
10. K H Kampert, M Unger, *Astroparticle Physics*, **35** (2012) 660.
11. A Aab et al**.** (Pierre Auger Collaboration), *Phys. Rev. D*, **90** (2014) 12.
12. Pierre Auger Collaboration (2021), Auger Open Data release 1-2021
13. D Heck et al., Report FZKA-6019 (1998), Forschungszentrum Karlsruhe.
14. S Ostapchenko, *Nucl. Phys. B. Proc. Suppl*. **151** (2006) 143.
15. H Fesefeldt, Report PITHA-85/02 (1985).
16. J N Capdevielle et al., "*The Karlsruhe Extensive Air Shower Simulation Code CORSIKA*", Kernforschungszentrum Karlsruhe, KfK (1992) 4998.
17. J Nishimura and K Kamata, *Prog. Theor. Phys*. **6** (1958) 93.
18. K Greisen, *Ann. Rev. Nucl. Part. Sci*. **10** (1960) 63.
19. A Aab et al. (Pierre Auger Collaboration), *Nucl. Instrum. Meth*. **798** (2015) 172.
20. T Antoni et al., *Astrop. Phys*. **24** (2005) 1.

21. P Bhattacharjee and G. Sigl, *Phys. Rep*. **327** (2000) 109.
22. J Abraham, et. al., (Pierre Auger collaboration) *Astroparticle Physics* **29** (2008) 243.
23. N Busca, D Hooper, and E W Kolb, *Phys. Rev. D* **73** (2006) 123001.
24. A Aab et al. (Pierre Auger Collaboration) *Phys. Rev. D* **91** (2015) 032003.